Accepted Manuscript

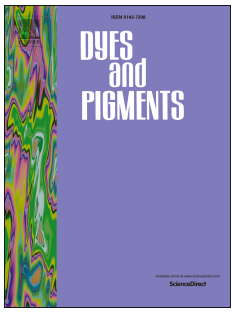

A highly selective two-photon probe with large turn-on signal for imaging endogenous HOCl in living cells

Jingjing Cao, Dong-Ming Jiang, Xin Ren, Ting Li, Xiao-Ting Gong, Yong-Rui Yang, Zhu-Guo Xu, Chun-Lin Sun, Zi-Fa Shi, Shengxiang Zhang, Hao-Li Zhang

PII: S0143-7208(17)30980-4

DOI: 10.1016/j.dyepig.2017.07.006

Reference: DYPI 6095

To appear in: *Dyes and Pigments*

Received Date: 28 April 2017

Revised Date: 30 June 2017

Accepted Date: 2 July 2017

Please cite this article as: Cao J, Jiang D-M, Ren X, Li T, Gong X-T, Yang Y-R, Xu Z-G, Sun C-L, Shi Z-F, Zhang S, Zhang H-L, A highly selective two-photon probe with large turn-on signal for imaging endogenous HOCl in living cells, *Dyes and Pigments* (2017), doi: 10.1016/j.dyepig.2017.07.006.

A Highly Selective Two-Photon Probe with Large Turn-On Signal for Imaging Endogenous HOCl in Living Cells

Jingjing Cao [a], Dong-Ming Jiang [a], Xin Ren [b], Ting Li [b], Xiao-Ting Gong [a], Yong-Rui Yang [a], Zhu-Guo Xu [a], Chun-Lin Sun [a], Zi-Fa Shi [a], Shengxiang Zhang [b,*] and Hao-Li Zhang [a,*]

[a] *State Key Laboratory of Applied Organic Chemistry (SKLAOC); Key Laboratory of Special Function Materials and Structure Design (MOE); College of Chemistry and Chemical Engineering, Lanzhou University, Lanzhou, 730000, P. R. China*

[b] *School of Life Sciences, Lanzhou University, Lanzhou 730000, P. R. China*

Tel: +86-0931-8912365 (H.Z.)

E-mail: haoli.zhang@lzu.edu.cn (H.Z.), sxzhang@lzu.edu.cn (S.Z.)

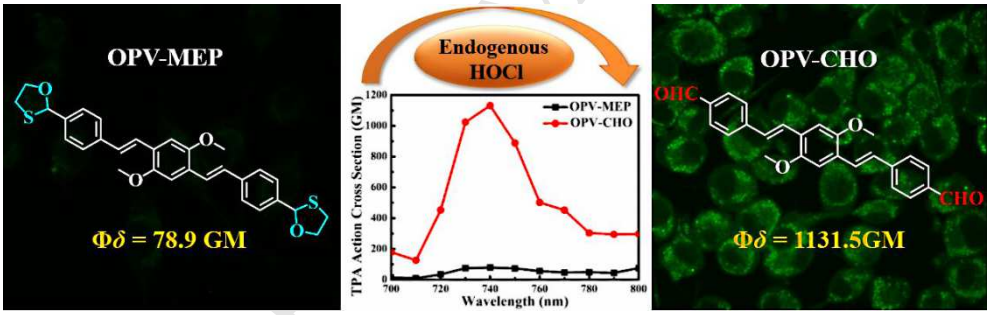

A Highly Selective Two-Photon Probe with Large Turn-On Signal for Imaging Endogenous HOCl in Living Cells

Jingjing Cao [a], Dong-Ming Jiang [a], Xin Ren [b], Ting Li [b], Xiao-Ting Gong [a], Yong-Rui Yang [a], Zhu-Guo Xu [a], Chun-Lin Sun [a], Zi-Fa Shi [a], Shengxiang Zhang [b,*] and Hao-Li Zhang [a,*]

[a] *State Key Laboratory of Applied Organic Chemistry (SKLAOC); Key Laboratory of Special Function Materials and Structure Design (MOE); College of Chemistry and Chemical Engineering, Lanzhou University, Lanzhou, 730000, P. R. China*

[b] *School of Life Sciences, Lanzhou University, Lanzhou 730000, P. R. China*

Tel: +86-0931-8912365 (H.Z.)

E-mail: haoli.zhang@lzu.edu.cn (H.Z.), sxzhang@lzu.edu.cn (S.Z.)

Abstract

Hypochlorous acid (HOCl) is one of the typical reactive oxygen species (ROS), which plays a crucial role in the immune system, and is involved in many neurodegenerative disorders, such as ischemic stroke, Alzheimer's, and Parkinson's disease. A two-photon probe for sensing HOCl with high selectivity, fast response (within 30 s), good penetration depth and low cytotoxicity is reported. Under two-photon excitation, the probe exhibited a remarkable fluorescence ‘‘turn-on’’ response to HOCl. Furthermore, the probe was successfully applied to the monitoring of endogenous HOCl stimulated by lipopolysaccharide in living microglia BV-2 cells.

Keywords: Two-photon fluorescent probe; Reactive oxygen species; Hypochlorous acid; Endogenous bio-imaging

1. Introduction

Reactive oxygen species (ROS) have recently received increasing attention due to their essential roles in various physiological and pathological processes [1-3], such as

anti-inflammatory regulation, pathogen response, cellular signaling, and aging [4-7]. Among the various ROS, hypochlorous acid (HOCl) generated from myeloperoxidase (MPO)-catalyzed peroxidation of chloride anions is a powerful antimicrobial agent contributing much in human immune defense system [8-10]. However, mounting evidence recently indicates that excessive accumulation of HOCl in living systems is implicated in neurodegenerative disorders [11], such as ischemic stroke , Alzheimer's, and Parkinson's disease [12-14]. Thus, it is highly desired to develop a fast and efficient method for monitoring HOCl in the presence of H_2O_2 and other ROS for an in-depth understanding of HOCl action mechanism in living organisms.

To date, many efforts have been made to develop HOCl fluorescent probes with different recognition moieties including oxime [15], thioester [16,17], dibenzoyl hydrazide [18], selenide [19,20] and other groups [21-23]; some of these probes have been successfully implemented in bio-imaging. However, many probes were based on conventional one-photon microscopy (OPM) and suffered shallow penetration depth limiting their biological applications *in vivo* and *in vitro*. Two-photon microscopy (TPM) is emerging as an effective tool for imaging in deep tissues due to its favorable properties, such as deep penetration, reduced photo-damage and photo-bleaching, lower background fluorescence and high observing resolution [24-27]. Unfortunately, two-photon absorption materials with large two-photon absorption action cross-section ($\Phi\delta$), a key factor representing their brightness under illumination, usually possess extended conjugated planar structures [28], which limited their cell permeability. Most of previously reported small molecule two-photon probes based on classical one-photon dyes exhibited high cell permeability but modest or small $\Phi\delta$ values, such as rhodamine, fluorescein, and coumarin [29]. Consequently, it is valuable to develop small molecule two-photon fluorescent probes with large two-photon action cross-section (above 1000 GM) for bio-imaging applications.

In this work, a two-photon probe **OPV-MEP** (Scheme 1) bearing two oxathiolane groups as the HOCl recognition sites and oligo (*p*-phenylene vinylene) (OPV) skeleton as the two-photon chromophore was synthesized. The oxidative deprotection of **OPV-MEP** by HOCl produces a compound **OPV-CHO** with large two-photon

absorption action cross-section (1131.5 GM). The **OPV-MEP** displays a fast and selective fluorescent turn-on response towards HOCl on two-photon excitation. Moreover, the probe was successfully utilized in two-photon imaging of endogenous HOCl in activated microglia BV-2 cells which can produce abundant HOCl in the cytoplasm. The cytotoxicity of the probe was also investigated.

2. Experimental Section

2.1. General information

All reagents were purchased without further purification and solvents were dried according to standard procedures before use. ^{1}H-NMR and ^{13}C-NMR spectra were performed on an INOVA-600 MHz instrument (Agilent) with TMS as internal standard. HRMS spectra were performed on a LTQ-Obitrap-ETD spectrometer. Absorption spectra were recorded on a T6 UV-vis spectrophotometer (Purkinje General). Fluorescence spectra were obtained on a FLS920 fluorimeter (Edinburgh Instruments). Various ROS including HOCl, ·OH, $^{1}O_2$, H_2O_2, $ONOO^-$, NO, TBO·, TBHP were prepared according to the procedure reported previously [30].

2.2. Synthesis of the probe

2.2.1. Synthesis of tetraethyl((2,5-dimethoxy-1,4-phenylene)bis(methylene))bis(phosphonate) (**2**)

1,4-Dimethoxybenzene (1.38 g, 10 mmol) was dissolved in 1,4-dioxane (250 mL) contained in the three-necked flask, then the solution was added with aqueous formaldehyde solution (35%, 5.8 g, 68 mmol). The reaction was processed by the gradual inlet of hydrogen chloride gas into the reactor at room temperature for 4 hours until the reaction was completed. Saturated sodium bicarbonate solution was added to the reaction mixture, and the product was extracted with dichloromethane. The organic layer was dried with anhydrous Na_2SO_4, followed by evaporation of the solvent. The crude product **1** was obtained as colourless crystals in 90% yield. MP: 155.8-157.2 °C. ^{1}H-NMR (600 MHz, $CDCl_3$), δ (ppm): 6.93 (s, 2H), 4.64 (s, 4H), 3.86 (s, 6H). ^{13}C-NMR (150 MHz, $CDCl_3$), δ (ppm): 151.16, 126.89, 113.42, 56.28, 41.26. HRMS (ESI): *m/z* calcd for $C_{10}H_{12}C_{l2}O_2^+$ $[M]^+$ 234.0209, found: 234.0211. IR

(KBr, cm^{-1}): 3437(w), 2968(m), 1738(w), 1510(s), 1462(s), 1410(s), 1320(m), 1223(s), 1037(s), 876(m), 737(m), 681(s), 608(m), 472(w).

Triethyl phosphite (29.13 g, 160 mmol) was added to the foregoing **1** (1.88 g, 8.0 mmol) contained within the flask and the solution was heated to 80 ℃ for 2 h. Then the crude product was purified by recrystallization with chloroform/hexane to afford **2** as colourless plate-like crystals in 86% yield. MP: 127.3-129.2 °C. ^{1}H-NMR (600 MHz, $CDCl_3$), δ (ppm): 6.91 (s, 2H), 4.05-4.00 (m, 8H), 3.80 (s, 6H), 3.22 (d, J = 20.4 Hz, 4H), 1.26-1.23 (m, 12H). ^{13}C-NMR (150 MHz, $CDCl_3$), δ (ppm): 151.00, 119.41, 114.04, 61.81, 56.10, 26.44 (d, $^{1}J_{CP}$ = 139.21 Hz), 16.27. HRMS (ESI): *m/z* calcd for $C_{18}H_{34}O_8P_2^+$ $[M+H]^+$ 439.1645, found: 439.1638. IR (KBr, cm^{-1}): 2985(s), 2839(m), 1520(s), 1414(m), 1271(s), 1215(s), 1049(s), 962(s), 883(m), 820(m), 631(m), 519(m).

2.2.2. Synthesis of 2,2'-(((1E,1'E)-(2,5-dimethoxy-1,4-phenylene)bis(ethene-2,1-diyl)) bis(4,1-phenylene))bis(1,3-oxathiolane) (**OPV-MEP**)

1,4-Phthalaldehyde (610 mg, 5.0 mmol) was dissolved in benzene (25 mL) in a two-necked flask, and the solution was added with 2-mercaptoethanol (390 mg, 5.0 mmol) and 4-methylbenzenesulfonic acid (33 mg, 0.20 mmol). The reaction was carried out in the Dean-Stark reactor at refluxing temperature to remove water for 3 hours. After cooling to room temperature, the mixture was added with diethyl ether (30 mL) and washed with saturated sodium bicarbonate solution (20 mL) and brine (20 mL) three times respectively. The organic layer was dried with anhydrous Na_2SO_4, followed by evaporation of the solvent to obtain crude 4-(1,3-oxathiolan-2-yl) benzaldehyde (**3**) as a yellow oil in 89% yield. ^{1}H-NMR (600 MHz, $CDCl_3$), δ (ppm): 10.02 (s, 1H), 7.88 (d, J = 7.8 Hz, 2H), 7.61 (d, J = 8.4 Hz, 2H), 6.12 (s, 1H), 4.57-4.54 (m, 1H), 4.04-4.00 (m, 1H), 3.30-3.21 (m, 2H). ^{13}C-NMR (150 MHz, $CDCl_3$), δ (ppm): 191.76, 146.35, 136.38, 129.91. 126.92, 86.01, 72.29, 34.06. HRMS (ESI): *m/z* calcd for $C_{10}H_{11}O_2S_1^+$ $[M+H]^+$ 195.0474, found: 195.0475. IR (KBr, cm^{-1}): 3383(w), 2872(m), 1697(s), 1608(s), 1387(m), 1302(m), 1203(s), 1066(s), 1016(m), 977(m), 806(s), 739(m), 480(w).

Sodium hydride (163 mg, 6.8 mmol) and **2** (296 mg, 0.68 mmol) were dissolved in

tetrahydrofuran (30 mL) in a two-necked flask, and the solution contained in two-necked flask was fulfilled with nitrogen atmosphere and cooled to 0 °C. Then the solution of **3** (269 mg, 1.4 mmol) in tetrahydrofuran (10 mL) was added to the reactor and the solution was stirred under 0 °C for 12 h. Crude product can be purified by extraction with dichloromethane and recrystallization with hexane/chloroform to obtain **OPV-MEP** as dark yellow powder in 68% yield. MP: 230.6-232.3 °C. ^{1}H-NMR (600 MHz, $CDCl_3$), δ (ppm): 7.55-7.45 (m, 10H), 7.13-7.10 (m, 4H), 6.07 (s, 2H), 4.57-4.54 (m, 2H), 3.99-3.94 (m, 2H), 3.93 (s, 6H), 3.32-3.28 (m, 2H), 3.23-3.20 (m, 2H). ^{13}C-NMR (150 MHz, $CDCl_3$), δ (ppm): 151.53, 138.25, 128.45, 126.95, 126.60, 123.65, 109.17, 86.90, 71.92, 56.35, 34.04. HRMS (ESI): *m/z* calcd for $C_{30}H_{31}O_4S_2^+$ $[M+H]^+$ 519.1658, found: 519.1665. IR (KBr, cm^{-1}): 3437(w), 2933(w), 2858(w), 1603(w), 1495(m), 1460(m), 1408(m), 1340(w), 1209(s), 1040(s), 968(m), 854(m), 812(w), 745(w), 692(w), 536(w).

2.3. Two-photon fluorescence measurement

Two-photon absorption cross-section was measured by a two-photon excited fluorescence method using rhodamine B as the reference. The femtosecond laser pulse from a Ti: sapphire system (690-850 nm, Tsunami) was used as the light source. All measurements were carried out in air at room temperature. Two-photon absorption cross-section was calculated by the following equation:

$$\delta = \delta_{\mathrm{ref}} \frac{\Phi_{ref}}{\Phi} \frac{c_{ref}}{c} \frac{n_{ref}}{n} \frac{F}{F_{ref}}$$

here the subscripts *ref* stands for the reference molecule. δ is the value of two-photon absorption cross-section; *c* is the solution concentration; *n* is the refractive index of the solution; *F* is the two-photon fluorescence integral intensities of the solution emitted at the exciting wavelength; and Φ is the fluorescence quantum yield. The δ_{ref} value of the reference is taken from the literature [31].

2.4. Cell cytotoxicity and imaging

To test the cytotoxicity of the probe **OPV-MEP**, MTT (5-dimethylthiazol-2-yl-2,5-diphenyltetrazolium bromide) assay was performed [32]. BV-2 cells were plated in 96-well flat-bottomed plates and incubated for 24 h at 37 °C

under 5% CO_2 prior to the **OPV-MEP** treatment. Then DMEM (Dulbecco's Modified Eagle Medium) with 10% FBS (Fetal Bovine Serum) was removed and replaced with fresh DMEM, and aliquots of **OPV-MEP** stock solutions (1 mM DMSO) were added to obtain final concentrations of 0.1, 1 and 10 μM, respectively. The treated cells were incubated for 24 h at 37 °C under 5% CO_2. Subsequently, cells were treated with 5 mg/mL MTT (40 μL/well) and incubated for an additional 4 h (37 °C, 5% CO_2). Then the cells were dissolved in the mixture of DMSO (150 μL/well), and the absorbance at 570 nm was recorded. The cell viability (%) was calculated according to the following equation:

$$\textit{Cell Viability} = OD_{570}(\textit{Sample}) / OD_{570}(\textit{Control})$$

where OD_{570} (Sample) represents the optical density of the wells treated with various concentration of **OPV-MEP** and OD_{570} (Control) represents that of the wells treated with DMEM plus 10% FBS. The percentage of cell survival values was relative to untreated control cells.

For two-photon bio-imaging, BV-2 cells were cultured in Dulbecco's modified Eagle's medium (DMEM) supplemented with 10% fetal bovine serum (FBS) (penicillin/streptomycin 100 μg/mL) at 37 °C in a humidified atmosphere with 5% CO_2 and 95% air. Cytoxicity assays showed that the **OPV-MEP** was safe enough for two-photon bio-imaging at low concentrations, so that the cells were incubated with 1 μM **OPV-MEP** at 37 °C under 5% CO_2 for 30 min. The cells were washed once and bathed in DMEM containing no FBS prior to imaging and/or HOCl addition. Then HOCl was added in the growth medium for 10 min at 37 °C, and the cells were washed three times with PBS buffer.

For the detection of endogenous HOCl, microglia BV-2 cells were cultured with 10% fetal bovine serum (FBS) (penicillin/streptomycin 100 μg/mL) exposed with 100 ng/mL LPS at 37 °C in a humidified atmosphere with 5% CO_2 and 95% air. Then the cells were incubated with 1 μM **OPV-MEP** at 37 °C under 5% CO_2 for 30 min, and washed 3 times with PBS buffer.

Two-photon fluorescence microscopy images of labelled cells were obtained on a FV1000MPE confocal microscope (Olympus) by exciting the probe with a

mode-locked titanium-sapphire laser source set at 740 nm.

3. Results and Discussion

3.1. Design and synthesis of probe **OPV-MEP**

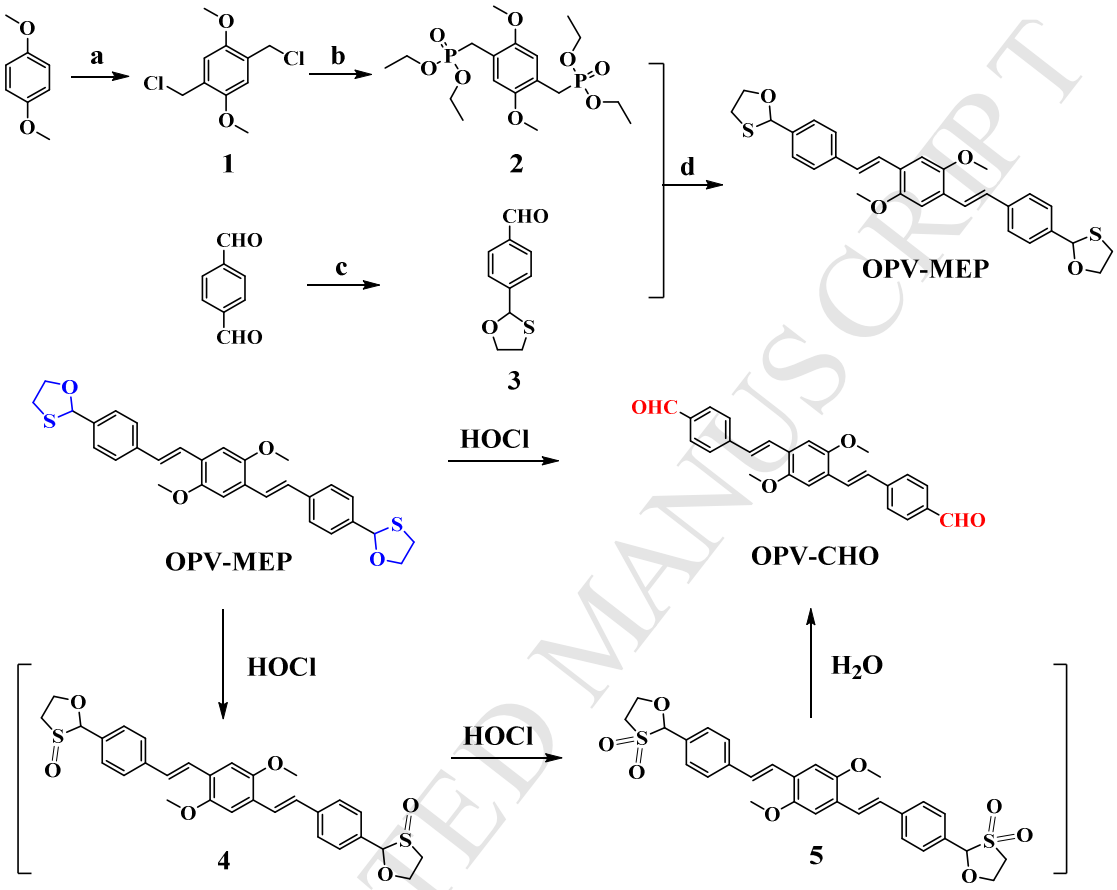

Scheme 1. Synthesis route and proposed sensing mechanism of **OPV-MEP**. Reagents and conditions: (a) HCHO, HCl, 1,4-dioxane, H_2O, r.t., 4 h; (b) triethyl phosphite, 80 °C, 2 h; (c) 2-mercaptoethanol, *p*-toluenesulfonic acid, benzene, reflux, 3 h; (d) NaH, THF, 0 °C, 12 h.

For two-photon materials, two-photon action cross-section is the key factor representing the two-photon fluorescence brightness [33]. Thus it was desired to design some small two-photon fluorescent probes with large two-photon action cross-section for HClO detection in biological systems. Toward this goal, we have designed a new small fluorescent probe with Oligo (*p*-phenylene vinylene) (OPVs) as the fluorescent skeleton. OPVs derivative are reported with a large two-photon active absorption cross-section and high fluorescence quantum yield and as well as good

photo-stability [34, 35]. Our previous research has suggested that the introduction of electron-donating and electron-withdrawing moieties into the OPVs molecule could significantly increase the two-photon absorption probability [36]. Based on this understanding, we designed aldehyde terminated OPV as TPA fluorescence dye. Protection of the two aldehyde groups using 2-mercaptoethanol would break D-π-A structure and produce the oxathiolane group which could be deprotected by HOCl to recover the aldehyde groups. We therefore used this mechanism to realize HOCl sensing.

The probe **OPV-MEP** was synthesized through four simple steps (Scheme 1) and characterized by ^{1}H NMR, ^{13}C NMR and HRMS (Fig. S1-S3). **OPV-MEP** was effectively prepared from reaction of precursor **2** and **3** with sodium hydride. The compound **3** was synthesized through the protection of commercially available compound 1,4-phthalaldehyde. The compound **2** was readily synthesized by 1,4-dimethoxybenzene and subsequent reaction of intermediate **1** with triethyl phosphite.

The proposed detection mechanism of probe **OPV-MEP** to HOCl was outlined in the Scheme 1, **OPV-MEP** is initially oxidized into intermediate sulfoxide compound **4** and sulphone compound **5** by HOCl, and finally hydrolyzed to generate **OPV-CHO** with cleavage of the oxathiolane rings. The probe can effectively respond to HOCl rather than other ROS, in good agreement with previous reported probes with thioether as recognition moieties [23,37-38]. Mass spectra was used to follow the deprotecion process of the oxathiolane group by HClO. A peak corresponding to [**OPV-CHO** + H]$^{+}$ appeared at m/z = 399.1599 after adding of HClO to the solution of **OPV-MEP**, which demonstrating the conversion of each of the oxathiolane groups into aldehyde moieties (Fig. S4).

3.2. Absorption and fluorescence properties of **OPV-MEP** for sensing HOCl

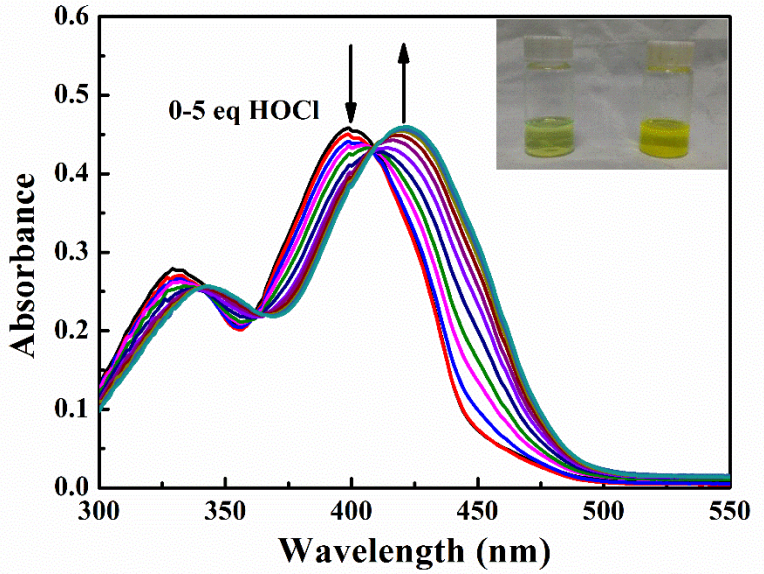

Fig. 1. UV-Vis titration spectra of **OPV-MEP** (10 μM) upon addition of HOCl (0-50 μM) in PBS/EtOH solution (PBS/EtOH = 1/1, v/v, pH 7.4, containing 0.25% THF). Inset: photographs of **OPV-MEP** solution before (left) and after (right) addition of HOCl in visible light.

The UV-Vis and one-photon fluorescent spectra of **OPV-MEP** were determined in PBS/EtOH solution buffered to physiological pH (0.1 M PBS, PBS/EtOH = 1/1, v/v, pH 7.4, containing 0.25% THF). The photophysical properties of the **OPV-MEP** and **OPV-CHO** were investigated and summarized in Table S1. As shown in Fig. 1, the UV-Vis spectrum of **OPV-MEP** exhibited the maximum absorption band centered at 400 nm (ε = 4.59 × 10^4 cm^{-1} mol^{-1}). Upon the addition of HOCl into the solution, the intensity of the absorption band at 400 nm decreased gradually, and a new absorption band centered at 420 nm occurred which was identical to the absorption spectrum of the supposed product **OPV-CHO** (Fig. S5). This red-shift (about 20 nm) of the maximum absorption band resulted from the expansion of the π-conjugate system, which could also be an evidence for the formation of aldehyde group. In addition, the color of **OPV-MEP** solution in visible light (shown in the inset of Fig. 1) turned from green to yellow after the addition of HOCl. The result displayed that the probe could be a colorimetric probe monitoring HOCl by direct visualisation.

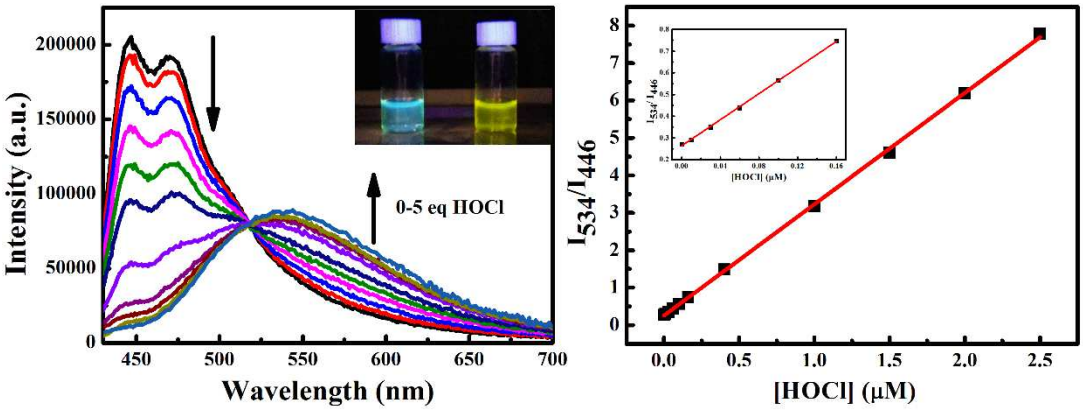

Fig. 2. Fluourescence titration spectra (a) and corresponding fluorescence intensity ratio (b) of 0.5 μM **OPV-MEP** upon the addition of HOCl (0- 2.5 μM) in PBS/EtOH solution (PBS/EtOH = 1/1, v/v, pH 7.4, containing 0.25% THF, λ_{ex}= 410 nm). Inset : (a) Change in the fluorescence of **OPV-MEP** before (left) and after (right) the addition of 50 μM HOCl, (b) the fluorescence intensity ratio by adding HOCl (0- 160 nM).

The fluorescence spectrum of **OPV-MEP** exhibited the maximum emission band centered at 446 nm under 410 nm excitation (Fig. 2). In order to evaluate the quantitative detection capacity of **OPV-MEP**, fluorescence titration experiments were carried out with the addition of HOCl (0-2.5 μM) into 0.5 μM probe in EtOH-PBS buffer solution (0.1 M PBS, PBS/EtOH = 1/1, v/v, pH 7.4, containing 0.25% THF). As shown in Fig. 2a, with the increasing amount of HOCl added into the solution from 0-2.5 μM, the fluorescence intensity at 446 nm decreased, and a new emission band centered at 534 nm appeared. Notably, there was a good linear relationship between the fluorescence intensity ratio (I_{534nm}/I_{446nm}) and the concentration of HOCl. Besides, the solution of **OPV-MEP** could be observed with a distinguishable fluorescence change from blue to yellow by direct visualization under 365 nm irradiation after the addition of HOCl. The result shows that **OPV-MEP** could make quantitatively responses towards HOCl at nanomolar level with high sensitivity. Furthermore, the response time of the probe to HClO was also investigated (Fig. S6), in which the **OPV-MEP** displayed fast and complete response towards HClO within 30 seconds.

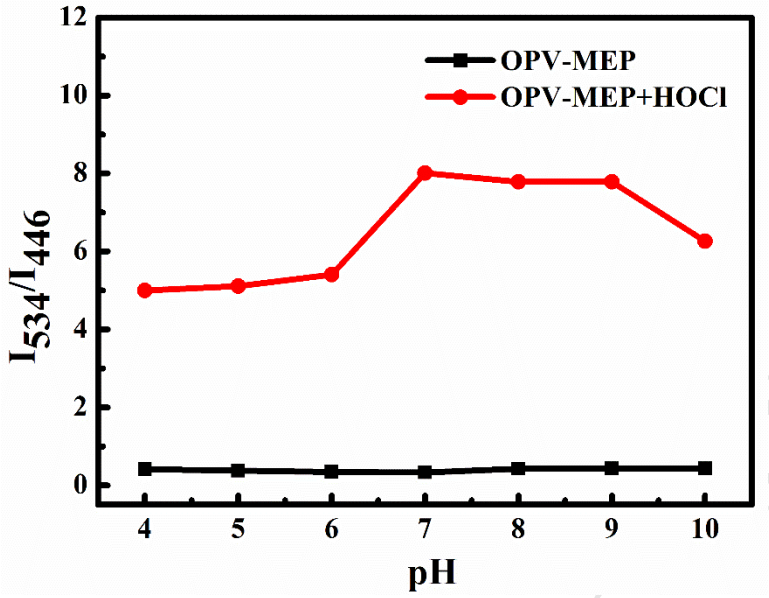

Fig. 3. The fluorescence spectra of **OPV-MEP** before and after the addition of HOCl in PBS/EtOH solution (pH 4 to 10).

In order to explore the detection effect of the probe in physiological pH, we also studied its response to HOCl in PBS/EtOH solution with different pH values ranging from 4 to 10. As shown in Fig .3, the fluorescence intensity of **OPV-MEP** kept a constant value at pH 4 to 10. After the addition of HOCl, the emission ratio (F_{534nm}/ F_{446nm}) became remarkably higher. These results demonstrate that the probe can response to HOCl over a broad pH range.

3.3. The selectivity

To investigate the selectivity of **OPV-MEP** to HOCl under physiological conditions, the fluorescence response of the probe was investigated with the addition of other competing ROS and reactive nitrogen species (RNS) in the same conditions. To a 0.5 μM solution of **OPV-MEP**, typical ROS and RNS including ·OH, $^1O_2$, H_2O_2, $ONOO^-$, NO, TBO· and TBHP were added respectively and the fluorescence spectra were recorded after 30 minutes. As shown in Fig.4, the addition of HOCl to **OPV-MEP** resulted in a remarkable change in fluorescence spectrum. However, **OPV-MEP** exhibited no response to other ROS and RNS, and even H_2O_2 as the precursor of HOCl also did not induce any observable fluorescence variation of the probe. Thus, **OPV-MEP** is confirmed to be a highly selective probe for HOCl

detection in biological system.

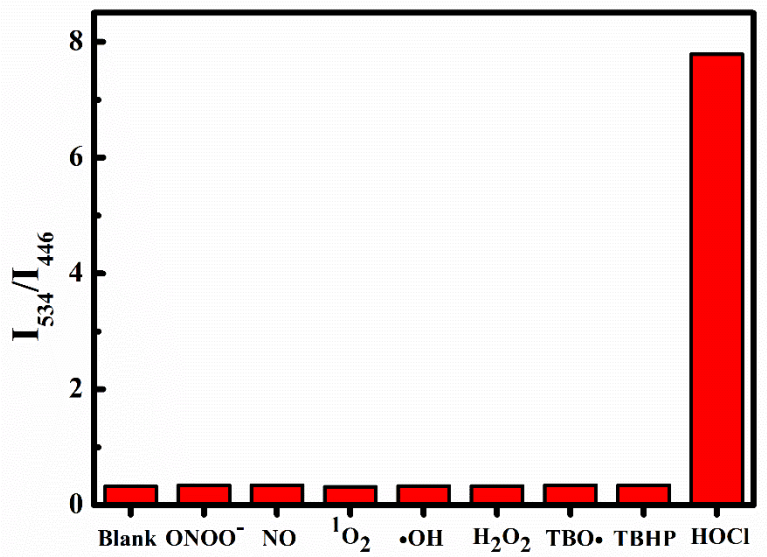

Fig. 4. Fluorescence ratio of probe **OPV-MEP** (0.5 μM) in response to HOCl (2.5 μM) and various ROS/RNS (2.5 μM) after 30 min in pH 7.4 PBS/EtOH (1:1, v/v, λ_{ex}= 400 nm, containing 0.25% THF).

3.4. Two-photon absorption properties

Most of the previously reported two-photon probes suffered with modest or small two-photon absorption action cross-section ($\Phi\delta$ usually less than 1000 GM), which greatly limit their practical application. Therefore, it was valuable to develop an efficient two-photon probe for monitoring HOCl with a large turn-on signal. In order to verify the capability of **OPV-MEP** as a two-photon probe, the two-photon absorption properties of **OPV-MEP** before and after the addition of HOCl were determined using two-photon excitation fluorescence method with rhodamine B as the reference. Two-photon absorption cross-section (δ) of **OPV-MEP** and **OPV-CHO** were determined in the wavelength range 700-800 nm in THF. As shown in Fig.5, over the measured range, the maximum TP action cross-section (δ_{max}) value of **OPV-MEP** is calculated to be 105.2 GM (1 GM= 10^{-50} cm^4 s·$photon^{-1}$) at 740 nm, while the δ_{max} value of the reaction product **OPV-CHO** is 2020.5 GM at 740 nm, which contributed to the electronic structure of OPV skeleton changed from "D–π–D–π–D" to "A–π–D–π–A". According to the fluorescence quantum yield of **OPV-MEP** and **OPV-CHO** were 0.75 and 0.56, the two-photon action cross-section of

OPV-MEP and **OPV-CHO** were calculated to be 78.9 GM and 1131.5 GM respectively. As a result, the two-photon action cross-section of the probe enhanced nearly 15-fold upon the addition of HOCl, which showed that **OPV-MEP** could serve as a two-photon "turn-on" probe for monitoring HOCl.

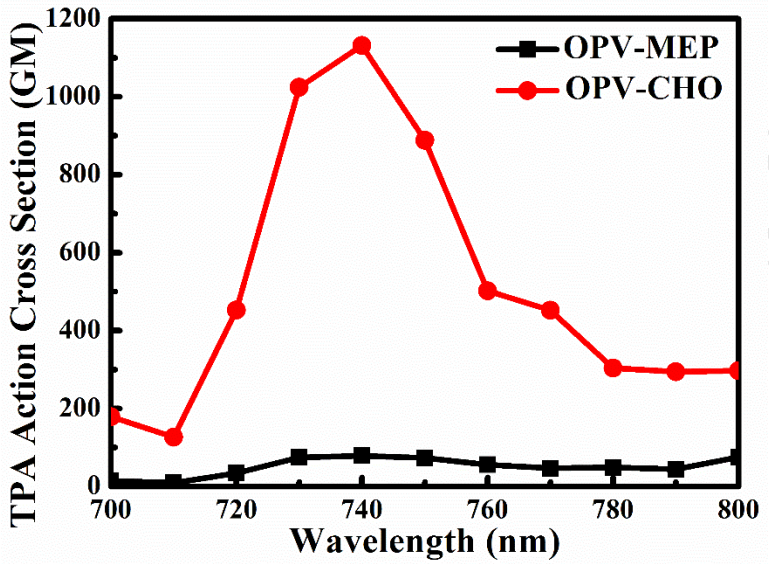

Fig. 5. Two-photon absorption action cross-section of **OPV-MEP** and reaction product **OPV-CHO** in THF solution

3.5. Cell imaging

Encouraged with the fast and highly selective response of the probe to HOCl, we then sought to evaluate its potential biological application in bio-imaging. To demonstrate the capability of **OPV-MEP** for the detection of HOCl in live cells upon two-photon excitation, murine BV-2 microglial cells were incubated with 1 μM **OPV-MEP** for 30 min at 37 °C in PBS buffer. As shown in Fig. 6(a-c), there were negligible fluorescence signal observed in the green emission channel of 490-540 nm for **OPV-MEP** under the excitation at 740 nm. After the addition of HOCl and incubation for another 10 minutes, intense fluorescence signals were emerged at the cytoplasm area of BV-2 cells, which indicated that **OPV-MEP** could be an effective tool for two-photon imaging of exogenous HOCl with good permeability in living cells. In addition, the bright-field images demonstrated that BV-2 cells were highly viable after treating with **OPV-MEP** during the imaging experiments, indicating relative low cytotoxicity of the probe towards living cells.

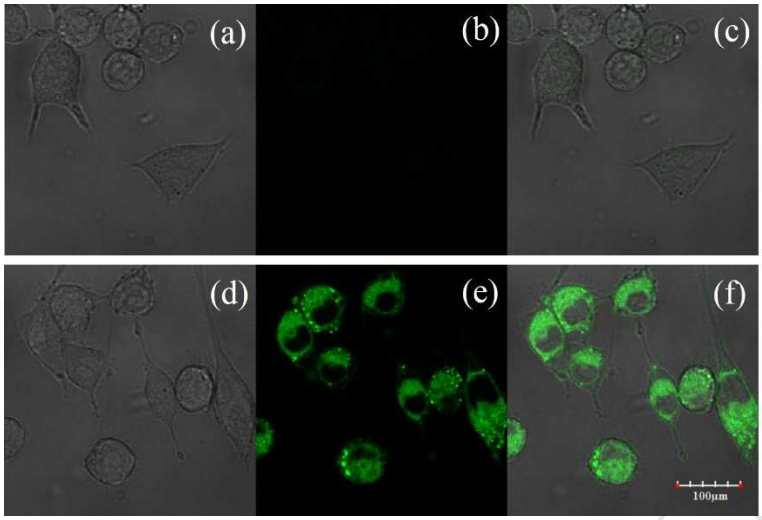

Fig. 6. Two-photon image of BV-2 cells incubated with **OPV-MEP** before (a-c) and after (d-f) addition of HOCl (λ_{ex} = 740 nm, green channel: 490- 540 nm). (a and d) Bright-Field images of the cells. (b and e) Fluorescence images of the cells. (c) The overlap of (a) and (b). (f) The overlap of (d) and (e).

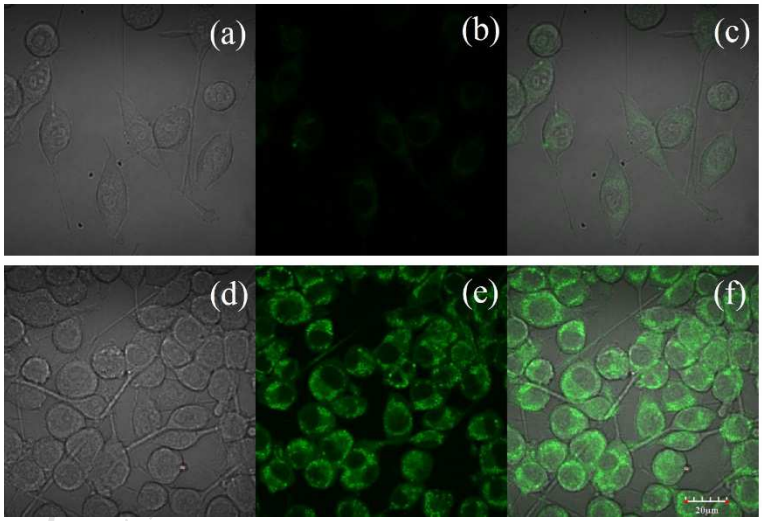

Fig. 7. Two-photon image of **OPV-MEP** in BV-2 cells incubated without (a-c) and with (d-f) the stimulation of LPS (λ_{ex}= 740 nm, green channel: 490- 540 nm). (a and d) Bright-Field images of the cells. (b and e) Fluorescence images of the cells. (c) The overlap of (a) and (b). (f) The overlap of (d) and (e).

To investigate the capability of **OPV-MEP** for the detection of endogenous HOCl, lipopolysaccharide (LPS) was employed as the stimulation reagent for generating HOCl in murine BV-2 microglial cells. The experiments were performed by incubating LPS stimulated cells with **OPV-MEP** for 30 min at 37 °C in PBS buffer.

Then the images of the cells were taken using TPM and clear fluorescence signal of the cells were observed at the optical window of 490-540 nm under 740 nm light excitation (Fig.7 d-f). In contrast, cells without the pre-treatment of LPS exhibited weak fluorescence signal as shown in Fig.7 a-c. Furthermore, two-photon fluorescence spectroscopy of LPS stimulated BV-2 cells were also investigated. After treatment of LPS for 48 h, **OPV-MEP** was added to the culture medium and the cells were incubated for another 30 min at 37 °C. As shown in Fig.7 d-f, two-photon fluorescence signal intensity of the probe in cytoplasm increased significantly after stimulated by LPS, compared to the one without LPS stimulation. Besides, it was clearly shown that a numeric enhancement of BV-2 cells was observed after LPS treatment, and no significant decrease in cell viability was observed.

3.6. Cell cytotoxicity

To demonstrate the practical use of **OPV-MEP** as a HOCl sensor for bio-imaging in living cells, the cytotoxicity of **OPV-MEP** was evaluated. MTT assay was conducted with different probe concentration ranging from 0.1 to 10 μM and BV-2 mouse microglia cell line was chosen for incubation. As shown in Fig. 8, more than 90% survival rate was observed, which showed great cell viability of **OPV-MEP**. The result indicated that **OPV-MEP** exhibited low cytotoxicity to BV-2 cells for 24 h incubation period. Therefore, the desired low cytotoxicity of **OPV-MEP** could render it safe to use for two-photon HOCl imaging in living cells.

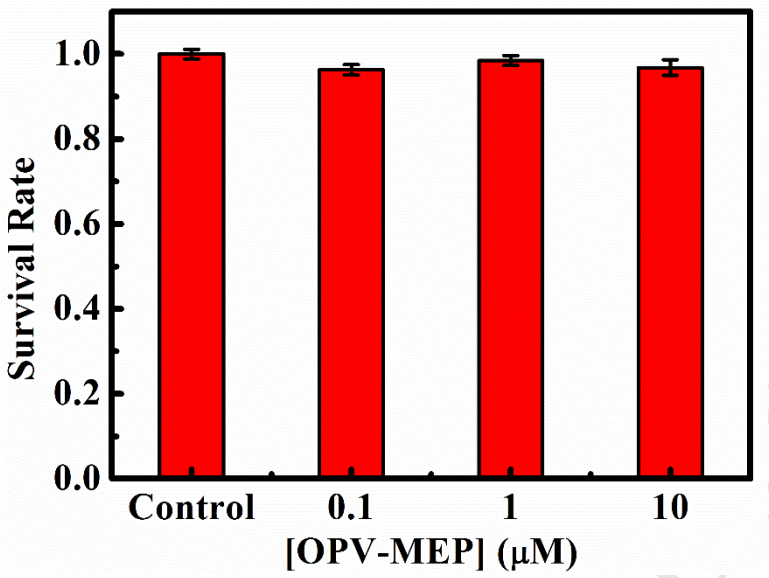

Fig. 8. Cell viability of BV-2 under different concentration of **OPV-MEP** for 24h.

4. Conclusions

In summary, we developed a new small molecule fluorescent probe **OPV-MEP** for monitoring hypochlorous acid based on the oligo (*p*-phenylene vinylene) two-photon platform. The addition of hypochlorous acid to **OPV-MEP** results in a large turn-on fluorescence signal in two-photon experiment. Furthermore, the probe displayed fast response, high selectivity for HOCl over other ROS as well as pH independence. Cell imaging experiments also confirmed the probe with good cell penetrability and low cytotoxicity. Benefited by these desired sensing properties and biocompatibility, the probe was successfully applied to the determination of exogenous and endogenous hypochlorous acid in living BV-2 cells for two-photon fluorescence imaging. We believe that **OPV-MEP** provides a promising tool to the further investigation of HOCl in biological research and clinical diagnoses.

Acknowledgments

The authors acknowledge the support from National Natural Science Foundation of China (NSFC. 51525303, 21602093, 31600831, 21572086), the Fundamental Research Funds for the Central Universities and 111 Project.

References

[1] Zhang JJ, Zhen X, Upputuri PK, Pramanik M, Chen P, Pu KY. Activatable photoacoustic nanoprobes for In vivo ratiometric imaging of peroxynitrite. Adv Mater 2017;29(6):1604764.

[2] Zhen X, Zhang CW, Xie C, Miao QQ, Lim KL, Pu KY. Intraparticle energy level alignment of semiconducting polymer nanoparticles to amplify chemiluminescence for ultrasensitive in vivo imaging of reactive oxygen species. ACS Nano 2016;10(6):6400-6409.

[3] Pu KY, Shuhendler AJ, Jokerst JV, Mei JG, Gambhir SS, Bao ZN, Rao JH. Semiconducting polymer nanoparticles as photoacoustic molecular imaging probes in living mice. Nature Nanotech 2014;9(3):233-239.

[4] Bauer G. Reactive oxygen and nitrogen species: efficient, selective, and interactive signals during intercellular induction of apoptosis. Anticancer Res 2000;20(6B):4115-4139.

[5] Finkel T, Holbrook NJ. Oxidants, oxidative stress and the biology of ageing. Nature 2000;408(6809):239-247.

[6] Chen XQ, Tian XZ, Shin I, Yoon J. Fluorescent and luminescent probes for detection of reactive oxygen and nitrogen species. Chem Soc Rev 2011;40(9): 4783-4804.

[7] Chen XQ, Wang F, Hyun JY, Wei TW, Qiang J, Ren XT, Shin I, Yoon J. Recent progress in the development of fluorescent, luminescent and colorimetric probes for detection of reactive oxygen and nitrogen species. Chem Soc Rev 2016;45(10):2976-3016.

[8] Lapenna D, Cuccurullo F. Hypochlorous acid and its pharmacological antagonism: An update picture. Gen Pharmacol 1996;27(7):1145−1147.

[9] Marcinkiewicz J,Chain B, Nowak B, Grabowska A, Bryniarski K, Baran J. Antimicrobial and cytotoxic activity of hypochlorous acid: interactions with taurine and nitrite. Inflamm Res 2000;49(6):280-289.

[10] Klebanoff SJ. Myeloperoxidase: friend and foe. J Leukoc Biol 2005;77(5):598-625.

[11] Pullar JM, Vissers MCM, Winterbourn CC. Living with a killer: the effects of

hypochlorous acid on mammalian cells. IUBMB Life 2000;51(4-5):259-266.

[12] Andersen JK. Oxidative stress in neurodegeneration: cause or consequence? Nat Med 2004;10(7):S18-S25.

[13] Yap YW, Whiteman M, Cheung NS. Chlorinative stress: An under appreciated mediator of neurodegeneration? Cell Signalling 2007;19(2):219-228.

[14] Jeitner TM, Kalogiannis M, Krasnikov BF, Gomlin I, Peltier MR, Moran GR. Linking Inflammation and Parkinson Disease: Hypochlorous Acid Generates Parkinsonian Poisons. Toxicol Sci 2016;151(2):388-402.

[15] Liang LJ, Liu C, Jiao XJ, Zhao LC, Zeng XS. A highly selective and sensitive photoinduced electron transfer (PET) based HOCl fluorescent probe in water and its endogenous imaging in living cells. Chem Commun 2016;52(51):7982-7985.

[16] Zhou J, Li LH, Shi W, Gao XH, Li XH, Ma HM. HOCl can appear in the mitochondria of macrophages during bacterial infection as revealed by a sensitive mitochondrial-targeting fluorescent probe. Chem Sci 2015;6(8):4884-4888.

[17] Zhang YR, Meng N, Miao JY, Zhao BX. A Ratiometric Fluorescent probe based on a through-bond energy transfer (TBET) system for imaging HOCl in living cells. Chem Eur J 2015;21(52):19058-19063.

[18] Ding SS, Zhang Q, Xue SH, Feng GQ. Real-time detection of hypochlorite in tap water and biological samples by a colorimetric, ratiometric and near-infrared fluorescent turn-on probe. Analyst 2015;140(13):4687-4693.

[19] Cheng GH, Fan JL, Sun W, Cao JF, Hu C, Peng XJ. A near-infrared fluorescent probe for selective detection of HClO based on Se-sensitized aggregation of heptamethine cyanine dye. Chem Commun 2014;50(8):1018-1020.

[20] Li GP, Zhu DJ, Liu Q, Xue L, Jiang H. A strategy for highly selective detection and imaging of hypochlorite using selenoxide elimination. Org Lett 2013;15(8):2002-2005.

[21] Wang BH, Chen D, Kambam S, Wang F, Wang Y, Zhang W, Yin J, Chen HY, Chen XQ. A highly specific fluorescent probe for hypochlorite based on fluorescein derivative and its endogenous imaging in living cells. Dyes Pigments 2015;120:22-29.

[22] Ma H, Song B, Wang YX, Liu CL, Wang X, Yuan JL. Development of organelle-targetable europium complex probes for time-gated luminescence imaging of hypochlorous acid in live cells and animals. Dyes Pigments 2017;140:407-416.

[23] Yuan L, Wang L, Agrawalla BK, Park SJ, Zhu H, Sivaraman B, Peng JJ, Xu QH, Chang YT. Development of targetable two-photon fluorescent probes to image hypochlorous acid in mitochondria and lysosome in live cell and inflamed mouse model. J Am Chem Soc 2015;137(18):5930-5938.

[24] Gao YT, Feng GX, Jiang T, Goh CC, Ng LG, Liu B, Li B, Yang L, Hua JL, Tian H. Biocompatible nanoparticles based on Diketo-Pyrrolo-Pyrrole (DPP) with aggregation-induced red/NIR emission for in vivo two-photon fluorescence imaging. Adv Funct Mater 2015;25(19):2857-2866.

[25] Kim D, Ryu HG, Ahn KH. Recent development of two-photon fluorescent probes for bioimaging. Org Biomol Chem 2014;12(26):4550-4566.

[26] Li L, Zhang CW, Chen GYJ, Zhu BW, Chai C, Xu QH, et al. A sensitive two-photon probe to selectively detect monoamine oxidase B activity in Parkinson's disease models. Nat Commun 2014;5:3276-85.

[27] Zhou L, Zhang X,Wang Q, Lv Y, Mao G, Luo A, et al. Molecular engineering of a TBET-based two-photon fluorescent probe for ratiometric imaging of living cells and tissues. J Am Chem Soc 2014;136:9838-9841.

[28] Kim HM, Cho BR. Two-photon materials with large two-photon cross sections. Structure-property relationship. Chem Commun 2009;2:153-164.

[29] H.M. Kim, B.R. Cho, Small-molecule two-photon probes for bioimaging applications, Chem. Rev. 115 (2015) 5014-5055.

[30] Wu GF, Zeng F, Wu SZ. A water-soluble and specific BODIPY-based fluorescent probe for hypochlorite detection and cell imaging. Anal Methods 2013;5(20): 5589-5596.

[31] Xu C, Webb WW. Measurement of two-photon excitation cross sections of molecular fluorophores with data from 690 to 1050 nm. J Opt Soc Am B 1996;13(3):481-491.

[32] Cheng D, Pan Y, Wang L, Zeng ZB, Yuan L, Zhang XB, Chang YT. Selective visualization of the endogenous peroxynitrite in an inflamed mouse model by a mitochondria-targetable two-photon ratiometric fluorescent probe. J Am Chem Soc 2017;139(1):285-292.

[33] Pawlicki M, Collins HA, Denning RG, Anderson HL. Two-Photon absorption and the design of two-photon dyes. Angew Chem Int Ed 2009;48(18):3244-3266.

[34] Gao F, Liao Q, Xu ZZ, Yue YH, Wang Q, Zhang HL, Fu HB. Strong two-photon excited fluorescence and stimulated emission from an organic single crystal of an Oligo(Phenylene Vinylene). Angew Chem Int Ed 2010;49(4):732-735.

[35] Pond SJK, Tsutsumi O, Rumi M, Kwon O, Zojer E, Bredas JL, Marder SR, Perry JW. Metal-ion sensing fluorophores with large two-photon absorption cross sections: aza-crown ether substituted donor-acceptor-donor distyryl benzenes. J Am Chem Soc 2004;126(30):9291-9306.

[36] Sun CL, Li J, Geng HW, Li H, Ai Y, Wang Q, Pan SL, Zhang HL. Understanding the unconventional effects of halogenation on the luminescent properties of Oligo(Phenylene Vinylene) molecules. Chem Asian J 2013;8(12):3091-3100.

[37] Xu Q, Lee KA, Lee S, Lee KM, Lee WJ, Yoon J. A highly specific fluorescent probe for hypochlorous acid and its application in imaging microbe-induced HOCl production. J Am Chem Soc 2013;135(26):9944-9949.

[38] Hawkins CL, Pattison DI, Davies MJ. Hypochlorite-induced oxidation of amino acids, peptides and proteins. Amino Acids 2003;25(3):259-274.

A Highly Selective Two-Photon Probe with Large Turn-On Signal for Imaging Endogenous HOCl in Living Cells

Jingjing Cao [a], Dong-Ming Jiang [a], Xin Ren [b], Ting Li [b], Xiao-Ting Gong [a], Yong-Rui Yang [a], Zhu-Guo Xu [a], Chun-Lin Sun [a], Zi-Fa Shi [a], Shengxiang Zhang [b,*] and Hao-Li Zhang [a,*]

[a] *State Key Laboratory of Applied Organic Chemistry (SKLAOC); Key Laboratory of Special Function Materials and Structure Design (MOE); College of Chemistry and Chemical Engineering, Lanzhou University, Lanzhou, 730000, P. R. China*

[b] *School of Life Sciences, Lanzhou University, Lanzhou 730000, P. R. China*

Tel: +86-0931-8912365 (H.Z.)

E-mail: haoli.zhang@lzu.edu.cn (H.Z.), sxzhang@lzu.edu.cn (S.Z.)

Highlights

- Large two-photon action cross-section of 1131.5 GM with small molecular weight.
- High specificity, fast response for HOCl fluorescence monitoring in a broad pH range.
- Selective imaging of endogenous HOCl in microglia BV-2 cells with low cytotoxicity.